基于 LabVIEW 的熔化极等离子弧焊接电弧电信号分析

白 岩, 高洪明, 路 浩, 石 磊
(哈尔滨工业大学 现代焊接生产技术国家重点实验室, 哈尔滨 150001)

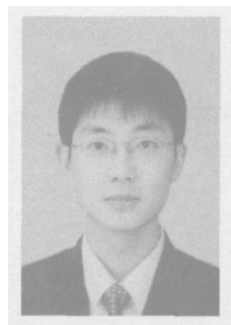

白 岩

摘 要: 在熔化极等离子弧焊接(plasma—MIG)试验系统基础上, 设计电流、电压信号采集系统, 对其电弧电特性信号进行采集, 用虚拟仪器软件 LabVIEW 对其进行处理, 得到 $U-t$, $I-t$, $U-I$ 相图。比较了熔化极等离子弧焊与常规熔化极气体保护焊电弧电信号的不同, 前者电流、电压波动很小, 后者波动很大; 研究了熔化极等离子弧焊接方法中 MIG 电流增大对电弧电信号的影响, 并对熔化极等离子弧焊接的不稳定电弧电信号进行了分析, 发现内弧对外弧的影响有一定规律性。

关键词: 熔化极等离子弧焊; 熔化极气体保护焊; 电弧电特性信号; 软件 LabVIEW
中图分类号: TG456 文献标识码: A 文章编号: 0253—360X(2006)08—059—04

0 序 言

熔化极等离子弧焊接方法由荷兰飞利浦公司的 Essers 和 Liefkens 等人于 1972 年发明的。这种焊接技术可以认为是等离子焊接和熔化极气体保护焊接方法的复合[1]。熔化极等离子弧焊接相对于传统的常规熔化极气体保护焊具有无飞溅、焊接过程稳定、质量好等优点, 尤其是熔敷速度高。1.2 mm 低碳钢焊丝通过 500 A 电流时, 可以获得 570 g/min 的熔敷速度[2~4]。

国外对于熔化极等离子弧焊接技术研究的比较早, 已取得了广泛的应用, 而国内则相对很少。作者建立稳定的熔化极等离子弧焊接试验系统, 在此基础上对电弧电特性信号进行采集、分析, 为该工艺的推广及应用奠定基础。

1 试验系统的建立

在试验室现有设备基础上, 设计建立了双电源、双气体、单回路水冷却的熔化极等离子弧焊接试验系统, 系统简图如图 1 所示。熔化极等离子弧焊接系统由 2 个独立电源组成, 因此使用 4 个传感器对其电弧电信号进行测量, 分别为等离子电压 U_p, MIG 电压 U_m, 等离子电流 I_p 和 MIG 电流 I_m。利用虚拟仪器软件 LabVIEW 对采集得到的数据进行分析、处理。

收稿日期: 2005—09—05
基金项目: 金属精密热加工国防科技重点实验室基金资助项目(03ZS6103)

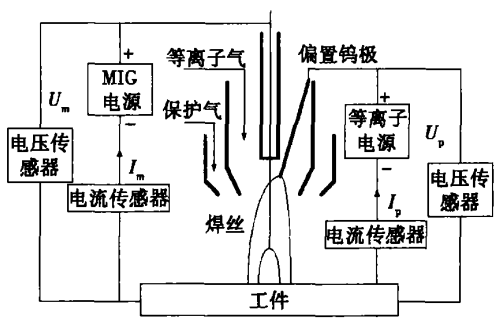

图 1 试验装置原理示意图

Fig. 1 Schematic diagram of experimental setup

2 试验结果及讨论

采集了获得良好焊缝时具有代表性的一系列参数下的熔化极等离子弧焊接电弧电信号, 并且采集了熔化极气体保护焊的电弧信号, 在对比中讨论前者电弧的特殊性。采集了熔化极等离子弧焊接中 MIG 电流逐渐增大时的电弧电信号, 并分析了对电弧信号的影响; 采集了熔滴由射滴过渡向射流过渡转变过程的电弧信号, 分析内弧与外弧的相互影响。

2.1 熔化极等离子弧与 MIG 电弧电特性对比分析

2.1.1 电流电压波形差别

宏观波形差别以电流波形对比为例。对于 MIG 焊, 当电压为 26.4 V, 电流为 230 A 时, 其 $I-t$ 图如图 2a 所示, 图 2a 为典型的短路过渡 $I-t$ 相图。对熔化极等离子弧焊来说, U_m 为 26.4 V, I_m 为 230 A, I_p 为 100 A 时的 I_m-t 图如图 2b 所示。从图 2a, b 对比可以看出, MIG 焊的电流波动很大, 电流波动范

围近 250 A，为短路过渡形式电流信号；熔化极等离子弧焊相对于常规的 MIG，加上了等离子电流，通过焊丝电流由大波动变至平稳，为稳定的射滴过渡。采集的电压宏观波形与此类似。为了更清楚地观察两种焊接方式波形的差异，在上述参数下，对 MIG 焊和熔化极等离子弧焊取 0.2 s 内的微观波形，以电压波形为例，对比如图 2c，d 所示。

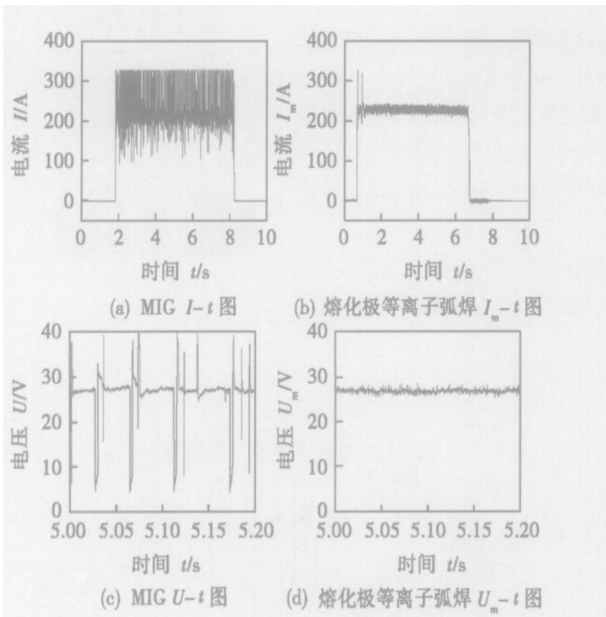

图 2 MIG 与熔化极等离子弧焊电流、电压波形差别

Fig. 2 Difference in waveforms of current and voltage between MIG welding and plasma-MIG welding process

宏观和微观电压与电流波形对比表明，相对于 MIG，熔化极等离子弧焊由于等离子电流的加入，增加了对焊丝的热输入，在通过焊丝相同电流下，熔滴过渡方式由短路过渡变为射滴过渡。

2.1.2 熔化极等离子弧与 MIG 电弧的 $U-I$ 相图差别

MIG 焊电压为 28.5 V，电流为 230 A 时，$U-I$ 相图如图 3a 所示，为典型的短路过渡[5]。对熔化极等离子弧焊，U_m 为 28.5 V，I_m 为230 A，I_p 为 100 A，时 U_m-I_m 相图如图 3b 所示。从图中可以看出，后者线簇变为集中团块状，说明电压电流集中在定值附近。左侧细竖线簇对应起弧、收弧阶段，空载电压很高，达 70 V 以上。从 U_m-I_m 相图分析，熔化极等离子弧焊接方法相对 MIG 来说加上了等离子电流，增加了热输入，熔滴过渡发生了变化，短路过渡频率变低或熔滴过渡方式由短路过渡变为射流过渡。

2.2 熔化极等离子弧中 MIG 电流对电弧电特性影响及分析

当 U_m 为 26.5 V，I_p 为 100 A 时，逐渐增大熔化极等离子弧焊中的 MIG 电流，采集电压、电流信号，并在试验中观察了相对应的过渡类型，见表 1。可以发现随着 MIG 电流增大，$U-I$ 相图由典型短路过渡形式转变为射流过渡形式(图 4)。

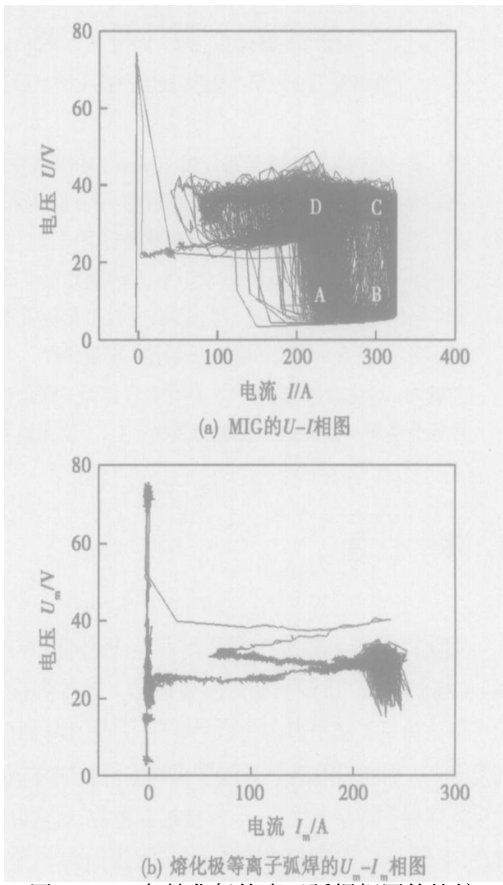

图 3 MIG 与熔化极等离子弧焊相图的比较

Fig. 3 Comparison of U-I phase graph between MIG welding and plasma-MIG welding process

表 1 MIG 电流增大对熔滴过渡类型的影响

Table 1 Influence of increase of MIG welding current on metal transfer forms

熔化极电流 I_m/A	过渡形式
200	短路过渡
215	大滴过渡
230	射流过渡

2.3 熔化极等离子弧焊内弧外弧的相互影响

熔化极等离子弧可视为等离子弧包围在 MIG 电弧周围的同轴复合电弧，MIG 弧为内弧，等离子弧为外弧，两弧之间的波动必然相互影响。

2.3.1 MIG 弧内发生短路过渡对等离子弧的影响

当 U_m 为 26.5 V，I_m 为 215 A，I_p 为 100 A 时，为一种临界过渡状态，出现不稳定的很短时间的短路过渡。截取 MIG 弧与等离子弧的 $U-t$ 和 $I-t$ 图 0.02 s 时段内的小窗口图像，如图 5 所示。

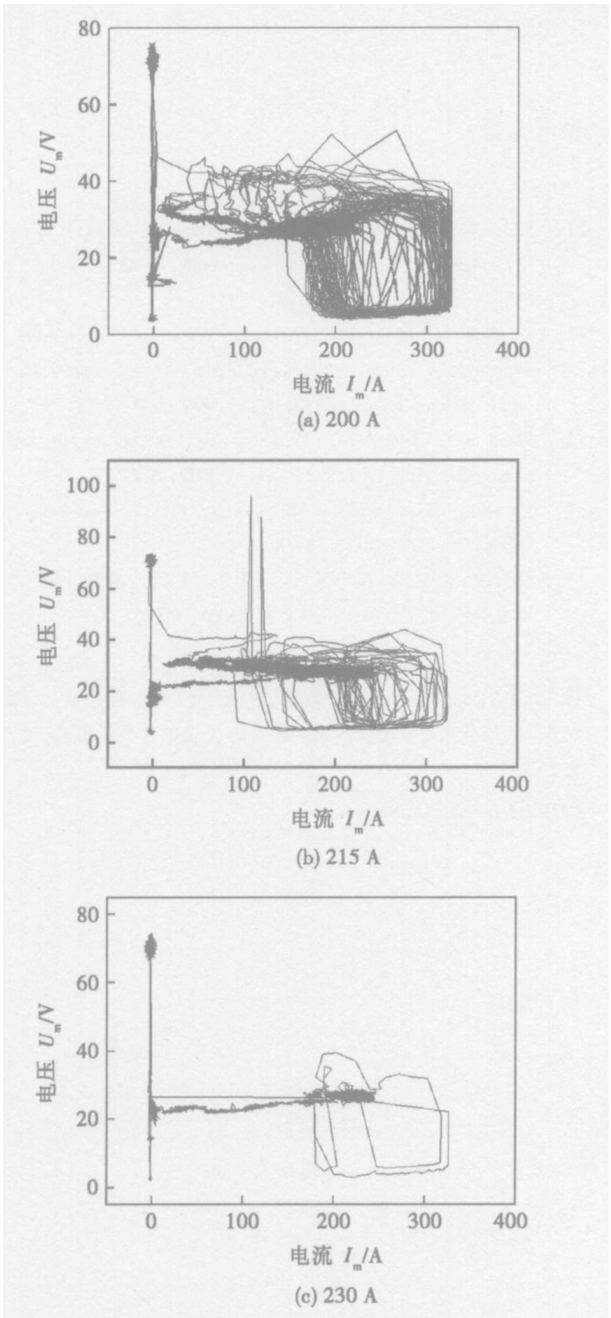

图 4　不同 MIG 电流下熔化极等离子弧焊 $U-I$ 相图

Fig. 4　$U-I$ phase graphs of plasma-MIG welding process with different MIG welding current

在 5.048 s 至 5.049 5 s 之间，MIG 电压由 26.5 V 降至 6 V 左右，MIG 电流由 215 A 升至 300 A，等离子弧电压由 26 V 升至 40 V，等离子电流保持 100 A 不变。在这个时间段内，熔化极等离子弧的内弧形成连接焊丝与工件的金属液柱。5.049 5 s 至 5.050 5 s之间，为电压恢复时间，MIG 电压由 6 V 升至 41 V，MIG 电流由 300 A 降至 150 A，等离子电压维持在 40 V，等离子电流保持 100 A 不变。在这个时间段内，内弧重新建立。

熔化极等离子弧的内弧发生短路过渡时，电弧导电能力下降，等离子焊接电源为恒流电源，为了保持等离子电流不变，等离子电压升高，才能保持与以前相同的导电能力。另一方面 MIG 电流不从熔化极等离子弧的主要导电通道外弧流过，而从焊丝与熔池之间形成的金属液柱流过，电磁收缩作用使等离子电压升高。

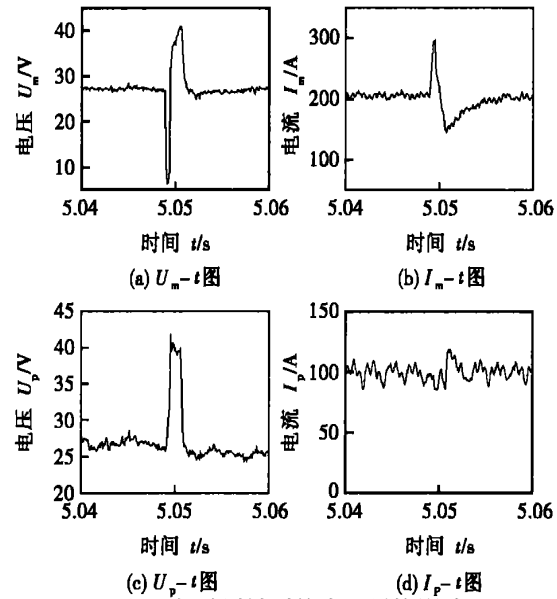

图 5　短路过渡对等离子弧的影响

Fig. 5　Effect of short circuiting transfer on plasma arc

2.3.2　MIG 电流下降对电弧影响

当 U_m 为 26.5 V，I_m 为 215 A，I_p 为 100 A 时，为一种临界过渡状态，分析此时不稳定电弧电信号时，发现 MIG 电流下降引起等离子电压升高，如图 6 所示。在 3.4 s 至 4.5 s 之间，MIG 电流由 215 A 下降

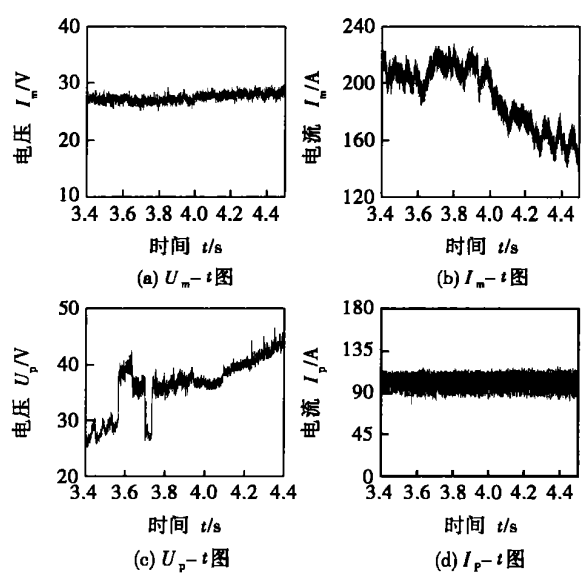

图 6　熔化极等离子弧焊中 MIG 电流下降对电弧信号影响

Fig. 6　Effect of decrease of MIG welding current on arc signals in plasma-MIG welding process

到 140 A, 等离子电压由 26 V 上升到 46 V, MIG 电压和等离子电流值几乎不变。MIG 电流下降, 电弧状态不稳定, 电弧导电能力下降。MIG 电源为恒压电源, 等离子电源为恒流电源, 它们极力维持 MIG 电压输出值和等离子电流输出值为定值, 这就需要电弧导电能力不受 MIG 电流下降的影响。因此等离子电压在 MIG 电流下降条件下升高。

3 结 论

(1) 熔化极等离子弧焊相对于常规 MIG 焊, 熔滴过渡发生了变化, 这说明等离子电流的存在改变了过渡方式, 克服了有飞溅的短路过渡方式, 为焊丝通过大电流创造了条件, 等离子电流的加入是实现高效焊接的关键。

(2) 熔化极等离子弧焊中内弧波动影响外弧, MIG 电流升高或下降破坏稳定的同轴复合双弧结构, 电弧导电能力发生改变, 引起等离子电压升高, 但是等离子电流不受 MIG 电流变化的影响, 保持稳定电流值。

参考文献:

[1] Essers W G, Liefkens A C. Plasma-MIG welding developed by philips [J]. Machinery and Production Engineering, 1972, 1(11): 632—633.

[2] Essers W G, Jelmorini G, Tichelaar G W. Arc characteristics and metal transfer with plasma-MIG welding[J]. Metal Construction and British Welding Journal, 1972, 4(12): 439—447.

[3] Essers W G, Jelmorini G, Tichelaar G W. The plasma-MIG welding process[J]. Philips Welding Reporter, 1972, 8(4): 1—7.

[4] Church J. What is plasma-MIG welding[J]. Canadian Welder and Fabricator, 1977, 68(1): 6—8.

[5] 许先果, 叶延洪, 周开庆, 等. 弧焊过程智能检测分析系统的建立与应用[J]. 中国机械工程, 2004, 15(15): 1362—1364.

作者简介: 白 岩, 男, 1980 年 12 月出生, 博士研究生。主要研究方向为熔化极等离子弧焊接工艺及焊接热过程数值模拟, 发表论文 2 篇。

Email: byyanhit@sina.com

ty, which makes the Young's modulus increase. If was found that the spraying orientation has effect on Young's modulus of coating which takes on the anisotropic property. In addition, interface fracture toughness was also introduced, which mainly include the 4-point bend test to measure interface critical strain energy rate, improved tensile test and local approach based on Weibull criterion.

Key words: coatings; Young's modulus; three-point bending; two-side coated specimen; interface fracture toughness

Analysis of plasma-MIG arc signal based on LabVIEW BAI Yan, GAO Hongming, Lu Hao, Shi Lei (State Key Lab of Advanced Welding Production Technology, Harbin Institute of Technology, Harbin 150001, China). p59—62

Abstract: The arc electrical signals were collected the data acquisition system in the plasma-MIG welding process, and the U-t、I-t、U-I diagrams analyzed with the Labview software were obtained. The difference of arc characteristic between plasma-MIG arc and MIG arc was studied and the effect of increase of MIG current on the electric signals of the Plasma-MIG arc was analyzed. The unstable arc electrical signals of Plasma-MIG were gathered and the result indicates that some contacts exist between inner arc and outer arc.

Key words: plasma-MIG; MIG; arc signal; LabVIEW

Mechanical properties of CO_2-laser and TIG aluminium alloy welded joint ZHOU Qinglin, QIAO Jisen, CHEN Jianhong, ZHU Liang(State Key Laboratory of Gansu Advanced Non-ferrous Metal Materials, Lanzhou University of Technology, Lanzhou 730050, China). p63—66

Abstract: The mechanical properties of Al-alloy 5A02 and its welded joint of CO_2 laser welding and TIG welding were studied. And rolling— orientation and rolling— uprightness orientation mechanical properties were measured. In addition, series load experiments were used to study properties of weld and base metal. This study considered that material anisotropy affects welded-joint mechanical properties, which is relate to each area materials mechanical properties of welded joint, will provide the theoretical bases for investigation of welded joint, as well as provide the local mechanical properties experimental data for crash simulation of Al-alloy automobile components.

Key words: CO_2 Laser welding; TIG welding; welded joint; anisotropy; curve fitting.

Extension of ductile fracture based on micro-plastic damage ZHU Zhijun, JING Hongyang, XU Lianyong, HUO Lixing(School of Materials Science and Engineering, Tianjin University, Tianjin 300072, China). p67—70

Abstract: Considering the inner micro plastic damage , using the finite element method (the computational cell model) and compiling the program to get parameters controlled ductile crack growth, the process of ductile fracture was simulated. The parameters to controll ductile crack growth were gotten from the simulating uniaxial tension test, which means that tests of the same material can be forecasted each other based the cell model. The results indicate that the prediction is in a good agreement with the experiment, and the cell model gives a good description of ductile crack growth. The prediction between different tests of the same material is reasonable.

Key words: plastic damage; finite element numerical simulation; experiment; ductile fracture

Analysis on high strength Al-Li alloy joints brazed in furnace ZHANG Ling, XUE Songbai, HAN Zongjie, HUANG Xiang (College of Materials Science and Technology, Nanjing University of Aeronautics and Astronautics, Nanjing 210016, China). p71—74

Abstract: High strength Al-Li alloy was brazed in furnace by using Ag-Al-Cu-Zn filler metal with CsF-AlF3 flux. The results show that under the condition of N_2 atmosphere, the tensile strength of butt joint is up to about 390 MPa with the strength factor of 0.89 and the shear strength of lap joint is up to about 380 MPa with the strength factor of 0.86, which all the strength factors are higher than those of fusion welding and brazed joints of high strength Al-Li alloy reported. The experimental results and theoretical analyses show that, effectively destroying and removing the complex oxide films on the surface of Al-Li alloy under the temperature of about 530℃ is the key factor to the brazing process and the protection of N_2 is an important way to improve mechanical properties of the braze metal.

Key words: high strength Al-Li alloy; furnace brazing; strength factor; fractograph

Methods of safe assessment for offshore pipeline LIU Mingliang, ZHANG Yufeng, HUO Lixing, DENG Caiyan(School of Material Science and Engineering, Tianjin University, Tianjin 30072, China). p75—78

Abstract: Given crack size and load, two methods of Structure Integrity Assessment Procedure(SINTAP) sponsored by the European Commission and BS910 were applied to assessment for welded joints of the API 5LX65 pipeline steel with surface flaw at the weld toe. The assessment was carried out according to Limit Load Solutions and the CTOD(Crack Tip Opening Displacement) test result. The failure lines of level 0 and level 1(level 1 and level 2 of BS7910) of the weld were derived from the tensile test results. The assessment showed that the assessment point is located within the failure line of analysis level 0 and level 1(level 1 and level 2 of BS7910). So welded joint of the pipeline is safe and the values obtained by using the two methods are very similar. Analysis of these two methods gives a help to use different methods for pipeline structure assessment. This study laid the foundation of choosing different methods of pipeline structure assessment.

Key words: offshore pipeline; stuctural integrity; failure assessment diagram